NIH Public Access
Author Manuscript
J Biol Chem. Author manuscript; available in PMC 2009 August 19.

Published in final edited form as:
J Biol Chem. 2008 January 4; 283(1): 603–612. doi:10.1074/jbc.M708250200.

Rho GTPase and cAMP/Protein Kinase A Signaling Mediates Myocilin-induced Alterations in Cultured Human Trabecular Meshwork Cells*

Xiang Shen‡, **Takahisa Koga**‡, **Bum-Chan Park**‡, **Nirmala SundarRaj**§, and **Beatrice Y. J. T. Yue**‡,1

‡Department of Ophthalmology and Visual Sciences, University of Illinois at Chicago College of Medicine, Chicago, Illinois 60612

§Department of Ophthalmology, University of Pittsburgh, Pittsburgh, Pennsylvania 15213

Abstract

Myocilin is a gene linked to the most common form of glaucoma, a major blinding disease. The trabecular meshwork (TM), a specialized eye tissue, is believed to be involved, at least in part, in the development of glaucoma. The myocilin expression is known to be up-regulated by glucocorticoids inTMcells, and an altered myocilin level may be the culprit in conditions such as corticosteroid glaucoma. Wild type myocilin, when transfected into cultured human TM cells, induced a dramatic loss of actin stress fibers and focal adhesions. Myocilin transfectants displayed a heightened sensitivity to trypsin. Adhesion to fibronectin, collagens, and vitronectin was compromised. The fibronectin deposition and the levels of fibronectin protein and mRNA were also reduced in myocilin transfectants. The fibronectin deposition could be restored by treatment with lysophosphatidic acid, a Rho stimulator. Assays further revealed that upon myocilin overexpression, the activity of RhoA was diminished, whereas the cAMP level and the protein kinase A (PKA) activity were augmented. Myocilin protein did not affect actin polymerization. The collapse of actin stress fibers and increased trypsin sensitivity from myocilin transfection could be reverted by co-expression of constitutively active RhoA or by treatment with PKA inhibitor H-89. The PKA activity, however, was not modified by co-expression of either constitutively active or dominant negative RhoA. These results demonstrate that myocilin has a deadhesive activity and triggers signaling events. cAMP/PKA activation and the downstream Rho inhibition are possible mechanisms by which myocilin in overabundance may lead to TM cell or tissue damage.

The trabecular meshwork (TM)[2] is a specialized tissue located at the chamber angle of the eye next to the cornea. It is composed of layers of trabecular beams made up of extracellular matrix (ECM) elements. TM cells that cover the beams display an endothelial cell-like morphology and lining property but are of a unique cell type (1,2). They are avid phagocytes (3), possess

*This work was supported by National Eye Institute, National Institutes of Health, Grants EY05628 and EY03890 (to B. Y. J. T. Y.), EY03263 (to N. S.), and Core Grant EY01792.

© 2008 by The American Society for Biochemistry and Molecular Biology, Inc.

1To whom correspondence should be addressed: Dept. of Ophthalmology and Visual Sciences, University of Illinois at Chicago, 1855 W. Taylor St., Chicago, IL 60612. Tel.: 312-996-6125; Fax: 312-996-7773; E-mail: beatyue@uic.edu.

[2]The abbreviations used are: TM, trabecular meshwork; ECM, extracellular matrix; IBMX, 3-isobutyl-1-methylxanthine; MMP, matrix metalloproteinase; PKA, protein kinase A; ca, constitutively active; dn, dominant negative; RT, reverse transcription; LPA, lysophosphatidic acid; GTPγS, guanosine 5′-3-*O*-(thio)triphosphate; GFP, green fluorescent protein; EGFP, enhanced GFP; DiI, 1,1′-dioctadecyl-3,3,3′,3′-tetramethyl-indocarbocyanine perchlorate.

NIH-PA Author Manuscript
NIH-PA Author Manuscript
NIH-PA Author Manuscript

NIH-PA Author Manuscript

NIH-PA Author Manuscript

NIH-PA Author Manuscript

contractile and migratory apparatus (4,5), have the capacity to produce ECM elements (2), and can transduce signals upon attachment to the ECM (6).

Immersed in the aqueous humor, the TM tissue is a major site for regulation of the aqueous outflow. Both the cells and the ECM in the TM may contribute to the flow resistance (2,7). It is believed that changes in the cell shape, volume, contractility, cell-matrix and cell-cell adhesion, and/or the quantity and composition of the ECM may affect the dimensions, direction, or resistance of the outflow pathway. High resistance to aqueous humor drainage may lead to elevated intraocular pressure and ultimately glaucoma, a heterogeneous disease generally characterized by neural loss and visual impairment.

Myocilin is the product of the *GLC1A* gene that has been linked directly to both juvenile and adult onset open angle glaucoma, the most common form of glaucoma (8). Multiple mutations have been identified in a number of families (8,9). Myocilin was initially identified as a 57-/55-kDa protein secreted into the medium of TM cultures after induction with glucocorticoids, such as dexamethasone (10). The myocilin mRNA and protein are present in a variety of ocular and nonocular tissues, including the retina and theTM(11). That myocilin expression can be induced dramatically by dexamethasone has been shown to be a distinct feature of TM cells (10,12). Myocilin, localized to both intracellular and extracellular sites in TM cells and tissue (11,13), is speculated to have diverse functions.

When up-regulated, myocilin may lead to pathology as is observed perhaps in cases of corticosteroid glaucoma (14). Evidence has also been provided that myocilin with mutations in the C terminus cannot be secreted. These mutants, in addition, suppress secretion of the wild type myocilin, resulting in intracellular accumulations (11,15,16).

An earlier report from our laboratory showed that transfection of myocilin into cultured human TM cells caused a loss of actin stress fibers and focal adhesions, compromising cell adhesion to fibronectin and cell spreading (17). In the present study, we further determined the biologic effects of myocilin. Specifically, the consequences of overexpressed myocilin on cell-matrix cohesiveness and matrix production in TM cells were investigated. The myocilin-induced events were shown to be mediated via Rho GTPase and cAMP/protein kinase A (PKA) signaling.

EXPERIMENTAL PROCEDURES

Cell Culture

Normal human eyes were obtained from the Illinois Eye Bank (Chicago, IL) or the National Disease Research Interchange (Philadelphia, PA). TM cells were derived from 11-, 21-, 22-, 32-, 33-, 43-, 46-, 47-, and 52-year-old donors without any known ocular diseases. The procurement of tissues was approved by the Institutional Review Board at the University of Illinois at Chicago in accordance with the Declaration of Helsinki. The TM tissues were dissected and cultured as previously described (18) on Falcon Primaria flasks (BD Biosciences) in complete medium that contained Dulbecco's modified Eagle's minimum essential medium, glutamine, 10% fetal bovine serum, 5% calf serum, and antibiotics. Second or third passaged cells were used for the study.

The TM cells displayed a polygonal morphology with a growth pattern distinct from that of fibroblastic and corneal endothelial cultures. They stained positively with DiI-acetylated low density lipoprotein (Invitrogen), consistent with previous reports that TM cells possess receptors for modified LDL (19–21). In parallel experiments, human umbilical vein endothelial cells (positive control) stained strongly, whereas human corneal fibroblasts (negative control) did not react with DiI-acetylated low density lipoprotein, as expected (data not shown).

NIH-PA Author Manuscript

NIH-PA Author Manuscript

NIH-PA Author Manuscript

Transfection of Constructs into TM Cells

Wild type myocilin was amplified by PCR using 5′-CCACCATGGCTATGAGGTTCTTCTGTGCACGTTGC-3′ antisense and 5′-TATCACATCTTGGAGAGCTTGATGTCATA-3′ sense primers. The 1.5-kilobase myocilin PCR product was subcloned using TA cloning into pTarget (Promega), a mammalian expression vector utilizing cytomegalovirus promoter and containing the neomycin gene for selection, to yield pTarget-myocilin. For construction of pMyocilin-EGFP, PCR was performed, and the EcoRI/BamHI-digested PCR product was cloned into pEGFP-N1 (BD Biosciences) at the corresponding sites. The expression plasmid (pOptineurin-EGFP) for optineurin, another glaucoma gene, was constructed as previously described (22). Sequencing was performed to determine the proper orientation and confirm the construct sequences.

pTarget-myocilin, pMyocilin-EGFP, or pOptineurin-EGFP was introduced into human TM cells using FuGENE 6 (Roche Applied Sciences) (17) or Lipofectamine Plus and Lifofectamine LTX (Invitrogen). TM cells were plated at 60% confluence 18 h before transfection. The vector/transfection reagent mixture was added to the cells for 24–48 h. As mock controls, TM cells were transfected in parallel with pTarget empty vector without the insert or vector pEGFP-N1.

In some experiments, TM cells were co-transfected with myocilin plasmids and RhoA expression vectors. Plasmids encoding constitutively active (ca) RhoA (V14 RhoA) and dominant negative (dn) RhoA (N19 RhoA) were gifts of Dr. Thomas Leung (IMCB, Singapore). For these vectors, human wild type RhoA was cloned into pcDNA3.1 at EcoRI and XbaI. The G14V or T19N mutation was introduced into RhoA via the QuikChange mutagenesis kit (Stratagene) to confer a ca or dn phenotype.

Western Blot Analysis

Transfected TM cells were incubated with serum-free Dulbecco's modified Eagle's minimum essential medium for 24 h. The media were collected, and TM cells were lysed in lysis buffer containing protease inhibitors (Roche Applied Science). The proteins in the lysate were quantified by Bradford protein assay using bovine serum albumin as a standard. Aliquots of lysates or medium (20 μg of protein equivalent) were subjected to 10% SDS-PAGE under reducing conditions. Western blotting was performed using polyclonal anti-myocilin (1:2000; a gift from Dr. Daniel Stamer, University of Arizona) (23) or anti-fibronectin (1:1000; BD Biosciences) and horseradish peroxidase-conjugated goat anti-rabbit IgG (1:10,000; Cappel). The protein bands were detected using SuperSignal Substrate from Pierce. Densitometric analysis was performed to measure the intensity of the myocilin or fibronectin bands with the use of 1D Image Analysis software from Eastman Kodak Co.

Relative Quantitative RT-PCR

Total RNA was isolated from TM cells using an RNeasy minikit (Qiagen), and cDNAs were prepared using random hexamers (SuperScript first strand synthesis system; Invitrogen). Relative quantitative RT-PCR was conducted using the QuantumRNA universal 18 S ribosomal RNA primer kit (Ambion) with myocilin sense (5′-ATGAGGTTCTTCTGTGCAACGTTGGCTGC) and antisense (5′-TCCAACCTCCTGGCCAGATTCTC) primers and a 1:4 ratio of 18 S primers to competimers or fibronectin sense (5′-GGTGGCTGTCAGTCAAAGCAAGC-3′) and antisense (5′-TGAGGCTGCGGTTGGTAAACAG-3′) primers and a 1:3 18 S primer/competimer ratio. The expected sizes of the myocilin, fibronectin, and 18 S RNA PCR products were 464, 771, and 315 bp, respectively. The RT step was omitted in negative controls. PCR products were resolved on agarose gels and quantified by densitometry. The level of myocilin or fibronectin transcript was normalized to the 18 S RNA product.

NIH-PA Author Manuscript

NIH-PA Author Manuscript

NIH-PA Author Manuscript

Cell-Matrix Adhesiveness Assay

CytoMatrix cell adhesion strips (Chemicon/Millipore) coated with ECM proteins, including fibronectin, vitronectin, and collagen types I and IV, were used. pTarget-myocilin-transfected TM cells were suspended from flasks using nonenzymatic dissociation buffer. 40,000 cells were added to each well of the rehydrated strips for a 45-min, 37 °C incubation. The unattached cells were removed, and the remaining ones were stained with 0.2% crystal violet in 10% ethanol. The dye associated with attached cells was solubilized for measurement of absorbance at 560 nm. Values were expressed as mean ± S.E. Student's *t* tests were used to analyze the statistical significance of the data. All assays were conducted in triplicate, and all experiments were repeated three times.

Trypsin Sensitivity

Mock and myocilin- or optineurin-transfected TM cells grown to confluence on 24-well plates were treated with Versene and incubated with 0.25% trypsin. Cell changes were monitored and photographed under a phase-contrast microscope. The time (mean ± S.D.) needed for the cells to shrink, round up, and break away from the bottom of the culture plate was determined (3).

Trypsin sensitivity was also examined using time lapse video microscopy. Cells were transfected with pEGFP-N1 and pMyocilin-EGFP or pOptineurin-EGFP for 24 h. The cells were observed under a Zeiss Axioscope (Carl Zeiss Micro-Imaging) using a × 40 objective. Images were captured before and every 30 s after the addition of 0.25% trypsin solution to the culture.

Immunofluorescence and Actin Staining

Transfected human TM cells were plated onto Lab-Tek CC2 glass chamber slides (Nalge Nunc International). Cells were fixed in either ice-cold methanol or paraformaldehyde-lysine-phosphate buffer, without or with permeabilization in 0.2% Triton X-100. After treatment of 3% H_2O_2 and blocking, the slides were incubated for 1 h with monoclonal anti-fibronectin or anti-vinculin (Chemicon). Normal mouse IgG was used as a negative control. The cells were further incubated with fluorescein isothiocyanate-goat anti-IgG or Cy3-goat anti-mouse IgG. Slides were mounted in Vectashield (Vector Laboratories) with 4′,6′-diamidino-2-phenylindole dihydrochloride. The staining was examined under a Leica confocal or a Zeiss 100M microscope. In some experiments, transfected cells were pretreated with 5 μM lysophosphatidic acid (LPA) for 16 h prior to the fibronectin staining.

The actin structure in normal untransfected and pTarget-myocilin-, pMyocilin-EGFP-, or pOptineurin-EGFP-transfected cells was examined using Oregon Green 488- or rhodamine-phalloidin (Molecular Probes). In some experiments, pMyocilin-EGFP-transfected cells were mixed with pDsRed-Monomer-C1 (BD Biosciences)-transfected ones in the same culture dishes, and the actin was stained with Alexa Fluor 350-phalloidin (Molecular Probes). pEGFP-N1- or pMyocilin-EGFP-transfected TM cells were also co-transfected with ca V14 or dn V12 RhoA. In other experiments, normal untransfected or pEGFP-N1- or pMyocilin-EGFP-transfected cells were treated overnight with cAMP-enhancing agent forskolin (50 μM; Sigma) or 3-isobutyl-1-methylxanthine (IBMX (500 μM); Sigma), or PKA inhibitor H-89 (10 nM; Calbiochem/EMD) before actin staining.

Zymography

11% SDS-polyacrylamide gels were prepared, and 1.5 mg/ml bovine skin gelatin was copolymerized in the gel (25). Aliquots of the culture media were loaded and electro-phoresed under nonreducing conditions. The SDS was removed, and the gel was incubated overnight in

NIH-PA Author Manuscript

NIH-PA Author Manuscript

NIH-PA Author Manuscript

a reaction buffer. After staining with Coomassie Brilliant Blue R-250, matrix metalloproteinase (MMP) activities were visualized against the stained background.

Pyrene Actin Polymerization Assay

The recombinant human myocilin was prepared as previously described (26). An actin polymerization assay was performed in triplicate using the actin polymerization biochemistry kit (Cytoskeleton). Briefly, G-buffer containing 9 μM pyrene-labeled actin and 0.2 mM ATP was prepared in 96-well plates. The reaction was started by adding a mixture of actin polymerization buffer and 30, 90, 300, or 900 nM or 9 μM myocilin to the wells. Bovine serum albumin (30 and 300 nM) was used as another control. Fluorescence change was measured at 1-min intervals using excitation of 340 nm and emission of 405 nm in a GENios Pro microplate reader (Tecan). Three independent experiments were performed.

Pull-down Assays for Active RhoA

Pull-down assays (Rho activation kit; Cytoskeleton) were performed to determine the GTP-bound Rho (27) using a glutathione *S*-transferase-rhotekin fusion protein containing the Rho binding domain as an affinity agent. pTarget mock- and pTarget-myocilin-transfected cells serum-starved for 18 h were lysed. The lysates were mixed at 4 °C with glutathione *S*-transferase-rhotekin (28) bound to Sepharose beads for 1 h. Proteins bound to the beads were resolved by 12% SDS-PAGE and immunoblotted with anti-RhoA (Santa Cruz Biotechnology). Cell lysates pre-incubated with GTPγS and GDP served as positive and negative controls, respectively. Prior to incubation with the beads, aliquots were removed from samples for total RhoA. Amounts of active GTP-RhoA that binds to glutathione *S*-transferase-rhotekin were normalized against amounts of total RhoA in the cell lysates, and the myocilin transfectant data (mean ± S.E.) were compared with controls. In some experiments, normal human TM cells were treated with forskolin (10 μM overnight) before the pull-down assay was performed.

cAMP and PKA Assays

The cAMP levels were measured using a cAMP enzyme immunoassay system (Promega) (29). TM cell lysates were assayed in triplicate, and the optical density was calculated against the standard curve to determine the cAMP level. Results from pTarget-myocilin transfectants were expressed as ratios (mean ± S.E.) relative to those of mock controls. The cAMP response was verified by treatment with forskolin.

Equal protein aliquots of lysates from TM cells transfected with pEGFP-N1, pTarget, pTarget-myocilin, and/or pMyocilin-EGFP without or with ca V14 or dn V12 RhoA were assayed for PKA activity (30). The activity was assessed by the incorporation of phosphate in Leu-Arg-Arg-Ser-Leu-Gly peptide using the nonradioactive Peptag system (Promega). Negative and positive controls were included, and the PKA activity was determined by densitometric analyses.

RESULTS

The myocilin construct pTarget-myocilin or pMyocilin-EGFP was introduced into human TM cells. After transfection, the levels of myocilin protein, as judged by Western blotting, as well as the transcript, as judged by relative quantitative RT-PCR, in myocilin transfectants were ~10–20-fold higher than those in mock controls (data not shown).

In agreement with results from our previous studies (17,31), the pMyocilin-EGFP-transfected green cells showed a marked loss of actin stress fibers (Fig. 1*A*) and vinculin-positive focal adhesions (Fig. 1*B*) compared with pEGFP-N1- and pOptineurin-EGFP-transfected controls as well as nontransfected cells. When present together in mixed cultures with pMyocilin-

NIH-PA Author Manuscript

NIH-PA Author Manuscript

NIH-PA Author Manuscript

EGFP-transfected TM cells (in *green*), the pDsRed-Monomer-C1-empty vector-transfected ones (in *red*) still displayed robust actin stress fibers although the actin dissolution was evident in the myocilin transfectants (Fig. 2). Meanwhile, the actin in the nontransfected cells in the mixed cultures remained intact.

pTarget mock-transfected TM cells adhered well, as anticipated (32), to fibronectin, vitronectin, and collagen types I and IV. After myocilin transfection, the ability of TM cells to adhere to these matrix proteins was significantly ($p < 0.0064$, $n = 3$) reduced (Fig. 3). To further examine the cell-matrix cohesiveness, TM cells were subjected to trypsin sensitivity tests. It was found that TM cells, upon myocilin transfection, became more sensitive to trypsinization. The trypsinization time needed to suspend cells from plates (Fig. 4*A*) was significantly ($p < 0.0001$) shorter for myocilin transfectants (92 ± 10.6 s, $n = 30$) than that for mock controls (144.7 ± 20.8 s, $n = 30$) or optineurin transfectants (136.5 ± 22.7 s, $n = 34$). Phase-contrast micrographs showed that compared with controls, the myocilin-transfected cultures had a greater number of cells rounding up and fewer cells remaining after treatment with trypsin for 120 s (Fig. 4*B*). Experiments using time lapse video microscopy in addition demonstrated that the myocilin-GFP-expressing cells, but not optineurin transfectants, rounded up sooner during trypsinization than the GFP control, indicating again increased trypsin sensitivity (Fig. 4*C*).

By immunofluorescence, the fibronectin deposition was seen diminished in pTarget-myocilin-transfected cultures (Fig. 5*A*). Cell density was similar in the control and myocilin-transfected specimens, and thus the decreased matrix assembly was not related to reduction in cell number. When treated with LPA, a Rho stimulator, the fibronectin (Fig. 5*A*) deposition in myocilin transfectants was enhanced. The matrix deposition appeared to be restored by the LPA treatment.

Western blotting detected a major 220 kDa band, immuno-reactive to anti-fibronectin, in the media of both mock-and pTarget-myocilin-transfected cultures. The level of the secreted fibronectin in the latter was only about one-third of that in the former (Fig. 5*B*). Consistent with the protein data, the relative level of fibronectin transcript, determined by relative quantitative RT-PCR, was also reduced by ~70% in myocilin transfectants (Fig. 5*C*). The zymographic pattern of TM cultures (Fig. 5*D*) was similar to that reported by Alexander *et al.* (31). A major gelatinase band with a 66-kDa molecular mass, identified previously as gelatinase A (33), was observed. Minor bands with higher and lower molecular masses might correspond to gelatinase B and the activated forms of gelatinase A, respectively. Overall, the MMP activities in myocilin transfectants were comparable with those in mock controls (Fig. 4*D*).

An *in vitro* actin polymerization assay was performed to determine whether the biologically active recombinant myocilin (26) expressed in a bacterial system affected actin polymerization. In positive controls, polymerization was observed to occur immediately following the addition of actin polymerization buffer (Fig. 6). A plateau was reached in ~25 min. Without the buffer, actin polymerization, as anticipated, failed to take place in negative controls. The actin polymerized at a nearly identical rate or kinetics as the positive controls regardless of whether recombinant human myocilin (90 n_M, 900 n_M, and 9 μ_M (Fig. 5); 30 and 300 n_M (data not shown)) or bovine serum albumin (30 and 300 n_M (data not shown)) was included in the actin polymerization buffer. The recombinant human myocilin had no impact on the actin polymerization *per se*.

Pull-down assays were carried out to measure the amounts of active RhoA in mock- and pTarget-myocilin-transfected cells. The level of GTP-bound or active RhoA in myocilin transfectants was lower (Fig. 7*A*) than that in controls. Quantitation by densitometry and

NIH-PA Author Manuscript

NIH-PA Author Manuscript

NIH-PA Author Manuscript

normalization to the total RhoA revealed that the RhoA activity upon myocilin transfection (0.55 ± 0.10, $n = 6$) was significantly ($p < 0.007$) reduced.

To determine whether the inhibition of RhoA was required for the myocilin-induced changes, TM cells were co-transfected with pMyocilin- EGFP and plasmid encoding ca V14 or dn N19 RhoA. As was demonstrated, untransfected (data not shown) or pEGFP-N1 mock-transfected cells exhibited long, prominent actin stress fibers (Fig. 7*B*) and abundant focal adhesions. Transfection with pMyocilin-EGFP alone caused a loss of actin stress fibers (Fig. 7*B*) and focal adhesions. Co-expression with dn N19 RhoA had little effect on the myocilin phenotype. In contrast, an increase of the actin (Fig. 7*B*) and focal adhesion (data not shown) assembly or an aversion of the myocilin phenotype was observed with ca V14 RhoA.

Regulation of Rho function has been shown to represent a major target for PKA in cytoskeletal modulation (34). Since PKA activity is dependent on cAMP, we explored whether the cAMP level and PKA activity were altered in myocilinoverexpressing TM cells. Assays performed indicated that the cAMP level (Fig. 8*A*; 1.47 ± 0.03 relative to mock controls, $n = 4$, $p < 0.0037$) and the PKA activity (Fig. 8*B*; 1.39 ± 0.002 relativse to mock controls, $n = 9$, $p < 0.0001$) were increased by 40–50% upon myocilin transfection. Inhibition of PKA by H-89 in pMyocilin-EGFP-transfected cells prevented, at least partially, the stress fiber dissolution (Fig. 8*C*). Time lapse video microscopy further demonstrated that both H-89 treatment and co-transfection with ca RhoA delayed the rounding up or prolonged the trypsinization time of myocilin-GFP-expressing cells (Fig. 8*D*).

Treatment of normal human TM cells with cAMP enhancing agents forskolin, an adenylate cyclase activator, and IBMX, an phosphodieseterase inhibitor, triggered a loss of actin stress fibers, fibronectin network, and focal adhesions (Fig. 9*A*). The forskolin effect could be counteracted by co-incubation of H-89 (Fig. 9*A*). Forskolin not only increased the cAMP level, as expected (Fig. 9*B*), but also reduced the RhoA activity (Fig. 9*C*). Furthermore, PKA activity in pTarget-myocilin-transfected TM cells remained elevated or was not modified by co-expression of either ca or dn RhoA (Fig. 9*D*). The PKA activity of pTarget-myocilin-transfected cells and those co-transfected with ca or dn RhoA was 1.39 ± 0.02 ($n = 9$), 1.44 ± 0.04 ($n = 3$), and 1.36 ± 0.03 ($n = 3$), respectively. cAMP/PKA therefore appeared to act upstream of RhoA signaling.

DISCUSSION

The present study demonstrates that myocilin, when overexpressed at a moderate level, induces a loss of actin stress fibers and focal adhesions (17), inhibits the adhesion of human TM cells to ECM proteins, and compromises the TM cell-matrix cohesiveness. These effects render the cells in a deadhesive state. Such a deadhesion phenomenon is similar to that associated with a group of matricellular proteins, including SPARC, thrombospondins, and tenascins, described extensively in the literature (35).

Similar to that found with matricellular proteins, such as tenascin-C (36), myocilin overexpression also blocks matrix assembly. Immunofluorescence experiments showed that the deposition of fibronectin (Fig. 5*A*) is diminished. The diminution is probably due to the gene regulation change at the transcriptional level, since a decrease in both the fibronectin protein and transcript levels were noted (Fig. 5, *B* and *C*). MMP activities, unaffected by the myocilin transfection (Fig. 5*D*), were perhaps not a major contributing factor to the alteration in the fibronectin assembly.

The fibronectin (Fig. 5*A*) deposition in myocilin-transfected cells was restored by treatment with LPA. Although capable of activating multiple signaling pathways, including pathways

NIH-PA Author Manuscript

NIH-PA Author Manuscript

NIH-PA Author Manuscript

involving phospholipase C and mitogen-activated protein kinase (37), LPA has been shown to particularly stimulate Rho-dependent pathways (38,39).

The change of actin structure, the lack of myocilin effect on actin polymerization, and the LPA restoration of matrix deposition (40) strongly suggest a possible role of the small GTPase Rho family in the deactivation process by myocilin. Rho GTPases cycle between the GDP-bound inactive and the GTP-bound active forms. When bound to GTP, they regulate cell behavior by binding to effector molecules and by altering their localization, protein-protein interactions, and activity. It is well documented that members of Rho family, especially RhoA, Rac1, and Cdc42 (41,42), coordinate many cellular responses, including adhesion and morphological change by regulating formation of different actin assemblies (43,44). For example, Rac1 triggers extension of lamellipodia and membrane ruffling, and Cdc42 induces outgrowth of peripheral spike-like filopodia. RhoA itself regulates formation of stress fibers and focal adhesions through activation of down-stream effectors, such as Rho kinase. RhoA also stimulates contractility mediated by activation of complexes of actin and myosin (45) and modulates ECM production (46) and assembly (47). Indeed, our investigation showed that subsequent to myocilin overexpression, RhoA activity is down-regulated. The involvement of Rho signaling is also verified by the demonstration that transfection of the ca but not the dn form of RhoA rescued the myocilin phenotype (Fig. 7*B* and Fig. 8*D*).

The cellular cAMP level is controlled by G protein-coupled receptors that couple to heterotrimeric G proteins to regulate adenylate cyclases, which catalyze cAMP formation, and by cyclic nucleotide phosphodiesterases, which hydrolyze cAMP. The classical intracellular effector of the cAMP signal is PKA, a tetramer consisting of two regulatory and two catalytic sub-units. Upon binding of cAMP to the regulatory subunit, the catalytic subunits dissociate and become available to phosphorylate cellular substrates (33,48).

The cAMP/PKA system plays a crucial role in many cellular mechanisms, such as cytoskeletal organization and adhesion in a cell type-specific manner (34). In human umbilical vein endothelial, vascular smooth muscle, and Chinese hamster ovary cells as well as astrocytes, agonists of cAMP/PKA signaling have been shown to cause dissolution of actin stress fibers and focal contacts (34,49). Elimination of surface- associated fibronectin (50) and myosin light chain dephosphorylation (51,52) have also been reported. In myocilin- overexpressing TM cells, disruption in cytoskeletal architecture and ECM deposition is found accompanying cAMP elevation and PKA activation. This finding is reminiscent of that in the above mentioned cell types. The overall increase of PKA activity in myocilin-overexpressing cells is modest. However, the subsequent demonstration that myocilin-induced changes can be averted by PKA inhibitor H-89 (Fig. 8, *C* and *D*) does support the view that the myocilin phenotype is, at least in part, related to the cAMP/PKA signaling. This is in keeping with a recent finding that a mild (20–30%) increase in total PKA activity after syndecan-2 overexpression was responsible for the induced filopodia formation and dendritic spinogenesis (53).

Normal human TM cells, after treatment with cAMP-enhancing agents forskolin and IBMX, showed a loss of actin stress fibers and focal adhesions as well as reduced fibronectin deposition (Fig. 9*A*). Reports in the literature have previously demonstrated an inhibition of RhoA activity by cAMP/PKA (54–56). In the current investigation, we found that stimulation of cAMP level by forskolin in normal TM cells led also to RhoA inhibition (Fig. 9*C*). Moreover, neither the ca nor the dn RhoA co-expression was able to modify the PKA activity (Fig. 9*D*) in myocilin transfectants, strongly suggesting that the RhoA acts downstream of cAMP/PKA signaling. It is unclear at present how the intracellular cAMP level is induced by the overexpressed myocilin. The possible target enzymes that lead to cAMP increase may include adenylate cyclases and phosphodiesterases.

NIH-PA Author Manuscript

NIH-PA Author Manuscript

NIH-PA Author Manuscript

In mixed cultures of myocilin-GFP- and DsRed-expressing cells, the actin stress fibers for the latter remain abundant, whereas the former, as expected, showed a dramatic actin loss (Fig. 2). Myocilin is known to be a secreted protein. The mixed culture result suggests that the secreted myocilin is not taken up by the cells and/or that it does not transmit a signal to induce actin changes. This notion is also supported by the observation that the nontransfected cells in the mixed cultures (Fig. 2) and the pMyocilin-EGFP-transfected cultures (Fig. 1*A*) have robust stress fibers.

A decrease in actin stress fibers and focal adhesions has been found to occur upon treatment with Rho kinase inhibitor Y-27632 (57,58) and gene transfer of dn RhoA (59) or C3 transferase (60) in TM cells. In the *in vivo* TM system, the actin cytoskeleton system has been linked to the regulation of the aqueous humor outflow (7,24). Experiments in living monkeys or perfusion organ cultures have shown that agents, such as cytochalasins, H-7, and latrunculins, which perturb the actin structure, increase the outflow facility. The increased flow is believed to result from the separation of cells from their neighboring cells and the ECM and the change in the overall TM geometry through cellular relaxation and contraction.

It is of note that those experiments with monkey and perfusion organ culture were all short term, from a few h to up to 7 days. On a long term and persistent basis, and especially because the TM cells *in situ* are continually subjected to stress from the aqueous flow and intraocular pressure fluctuations, it is conceivable that the altered actin cytoskeleton and impaired cell-matrix adhesiveness observed with overexpressed myocilin would ultimately weaken the TM cells and destabilize the system. Cell loss and pathologic consequences may then ensue. The vulnerability of myocilin-transfected TM cells has been implicated by their susceptibility to apoptotic challenge (17). Evidence was presented that anti-Fas treatment triggered a significantly higher level of apoptosis in myocilin transfectants than the mock controls (17).

Based on our results, we propose a schematic model in Fig. 10.Wesurmise that moderately up-regulated myocilin elevates cAMP, which leads to PKA activation and RhoA inactivation, and in turn triggers the loss of actin stress fibers, focal adhesions, matrix deposition, and cell-matrix cohesiveness in TM cells. Through these steps and/or other pathways, cells may become vulnerable to develop pathology upon additional stress. The involvement of the cAMP/PKA and RhoA GTPase, demonstrated in the current study, constitutes a novel observation and suggests a mechanism by which myocilin may induce cell or tissue damage.

Acknowledgment

We thank Ruth Zelkha for expert imaging.

REFERENCES

1. Bill A. Invest. Ophthalmol. Vis. Sci 1975;14:1–3.
2. Yue BYJT. Surv. Ophthalmol 1996;40:379–390. [PubMed: 8779084]
3. Zhou L, Fukuchi T, Kawa JE, Higginbotham EJ, Yue BYJT. Invest. Ophthalmol. Vis. Res 1995;36:787–795.
4. Calthorpe CM, Grierson I. Exp. Eye Res 1990;51:39–48. [PubMed: 2373179]
5. Stumpff F, Wiederholt M. Ophthalmologica 2000;214:33–53. [PubMed: 10657743]
6. Zhou L, Cheng EL, Rege P, Yue BYJT. Exp. Eye Res 2000;70:457–465. [PubMed: 10865994]
7. Tian B, Peters DM, Kaufman PL. Curr. Opin. Ophthalmol 2006;17:168–174. [PubMed: 16552252]
8. Stone EM, Fingert JH, Alward WL, Nguyen TD, Polansky JR, Sunden SLF, Nishimura D, Clark AF, Nystuen A, Nichols BE, Mackey DA, Ritch R, Kalenak JW, Craven EE, Sheffield VC. Science 1997;275:668–670. [PubMed: 9005853]

NIH-PA Author Manuscript

NIH-PA Author Manuscript

NIH-PA Author Manuscript

9. Gong G, Kosoko-Lasaki O, Haynatzki GR, Wilson MR. Hum. Mol. Genet 2004;13:R91–R102. [PubMed: 14764620]
10. Nguyen T, Chen P, Huang W, Chen H, Johnson D, Polansky J. J. Biol. Chem 1998;273:6341–6350. [PubMed: 9497363]
11. Tamm ER. Prog. Retin. Eye Res 2002;21:395–428. [PubMed: 12150989]
12. Wentz-Hunter K, Shen X, Yue BYJT. Mol. Vis 2003;9:308–314. [PubMed: 12847420]
13. Ueda J, Wentz-Hunter K, Cheng EL, Fukuchi T, Abe H, Yue BYJT. J. Histochem. Cytochem 2000;48:1321–1329. [PubMed: 10990486]
14. Clark AF. J. Glaucoma 1995;4:354–369.
15. Caballero M, Rowlete LL, Borras T. Biochim. Biophys. Acta 2000;1502:447–460. [PubMed: 11068187]
16. Jacobson N, Andrews M, Shepard AR, Nishimura D, Searby C, Fingert JH, Hageman G, Mullins R, Davidson BL, Kwon YH, Alward WLM, Stonex EM, Abbott AF, Sheffield VC. Hum. Mol. Genet 2001;10:117–125. [PubMed: 11152659]
17. Wentz-Hunter K, Shen X, Okazaki K, Tanihara H, Yue BYJT. Exp. Cell Res 2004;297:39–48. [PubMed: 15194423]
18. Yue BYJT, Higginbotham E, Chang I. Exp. Cell Res 1990;187:65–68. [PubMed: 2298262]
19. Chang IL, Elner SG, Yue BYJT, Cornicelli JA, Kawa JE, Elner VM. Curr. Eye Res 1991;10:1101–1112. [PubMed: 1802612]
20. Stamer WD, Roberts BC, Howell DN, Epstein DL. Invest. Ophthalmol. Vis. Sci 1998;39:1804–1812. [PubMed: 9727403]
21. Park BC, Tibudan M, Samaraweer M, Shen X, Yue BYJT. Genes Cells 2007;12:969–979. [PubMed: 17663725]
22. Park BC, Shen X, Samaraweera M, Yue BYJT. Am. J.Pathol 2006;169:1976–1989. [PubMed: 17148662]
23. Hardy KM, Hoffman EA, Gonzalez P, McKay BS, Stamer WD. J. Biol. Chem 2005;280:28917–28926. [PubMed: 15944158]
24. Tian B, Geiger B, Epstein DL, Kaufman PL. Invest. Ophthalmol.Vis. Sci 2000;41:619–623. [PubMed: 10711672]
25. Ando H, Twining SS, Yue BYJT, Zhou X, Fini ME, Kaiya T, Higginbotham EJ, Sugar J. Invest. Ophthalmol. Vis. Sci 1993;34:3541–3548. [PubMed: 7505006]
26. Park BC, Shen X, Fautsch MP, Tibudan M, Johnson DH, Yue BYJT. Mol. Vis 2006;12:832–840. [PubMed: 16902400]
27. Vouret-Craviari V, Bourcier C, Boulter E, van Obberghen-Schilling E. J. Cell Sci 2002;115:2474–2484.
28. Ren XD, Kiosses WB, Schwartz MA. 1999;18:578–585.
29. Forster ML, Sivick K, Park Y, Arva P, Lencer WI, Tsai B. J. Cell Biol 2006;173:853–859. [PubMed: 16785320]
30. Darmond O, Bezzi M, Mariotti A, Ruegg C. J. Biol. Chem 2002;277:45838–45846. [PubMed: 12237321]
31. Sakai H, Park BC, Shen X, Yue BYJT. Invest. Ophthalmol.Vis. Sci 2006;47:4427–4434. [PubMed: 17003436]
32. Zhou L, Zhang S, Yue BYJT. Invest. Ophthalmol. Vis. Res 1996;37:104–113.
33. Alexander JP, Samples JR, van Buskirk EM, Acott TS. Invest. Ophthalmol. Vis. Res 1991;32:172–180.
34. Howe AK. Biochim. Biophys. Acta 2004;1692:159–174. [PubMed: 15246685]
35. Bornstein P, Sage EH. Curr. Opin. Cell Biol 2002;14:608–616. [PubMed: 12231357]
36. Midwood KS, Schwarbauer JE. J. Cell Biol 2002;13:3601–3613.
37. Lee CW, Nam JS, Park YK, Choi HK, Lee JH, Kim NH, Cho J, Song DK, Suh HW, Lee J, Kim YH, Huh SO. Biochem. Biophys. Res. Commun 2003;305:455–461. [PubMed: 12763014]
38. van Leeuwen FN, Giepmans BN, van Meeteren LA, Moolenaar WH. Biochem. Soc. Trans 2003;31:1209–1212. [PubMed: 14641027]

NIH-PA Author Manuscript

NIH-PA Author Manuscript

NIH-PA Author Manuscript

39. Weiner JA, Fukushima N, Contos JJ, Scherer SS, Chun J. J. Neurosci 2001;21:7069–7078. [PubMed: 11549717]
40. Hall A. Annu. Rev. Cell Biol 1994;10:31–54. [PubMed: 7888179]
41. Mackay DJG, Hall A. J. Biol. Chem 1998;273:20685–20688. [PubMed: 9694808]
42. Nobes CD, Hall A. Cell 1995;81:53–62. [PubMed: 7536630]
43. Burridge K, Wennerberg K. Cell 2004;116:167–179. [PubMed: 14744429]
44. Tapon N, Hall A. Curr. Opin. Cell Biol 1997;9:86–92. [PubMed: 9013670]
45. Kato M, Iwamoto H, Higashi N, Sugimoto R, Uchimura K, Tada S, Sakai H, Nakamuta M, Nawata H. J. Hepatol 1999;31:91–99. [PubMed: 10424288]
46. Schoenwaelder SM, Burridge K. Curr. Opin. Cell Biol 1999;11:274–286. [PubMed: 10209151]
47. Pereira M, Rybarczyk BJ, Odrljin TM, Hocking DC, Sottile J, Simpson-Haidaris PJ. J. Cell Sci 2002;115:609–617. [PubMed: 11861767]
48. Taylor SS. J. Biol. Chem 1989;264:8443–8446. [PubMed: 2656679]
49. Lampugnani MG, Giorgi M, Gaboli M, Dejana E, Marchisio PC. Lab. Invest 1990;63:521–531. [PubMed: 2172648]
50. Smirnov VN, Antonov AS, Antonova GN, Romanov YA, Kabaeva NV, Tchertikhina IV, Lukashev ME. J. Mol. Cell Cardiol 1989;21:3–11. [PubMed: 2543828]
51. Kreisberg JI, Ghosh-Choudhury N, Radnik RA, Schwartz MA. Am. J. Physiol 1997;273:F283–F288. [PubMed: 9277589]
52. Srinivas SP, Satpathy M, Guo Y, Anandan V. Invest. Ophthalmol. Vis. Sci 2006;47:4011–4018. [PubMed: 16936117]
53. Lin Y-L, Lei Y-T, Hong C-J, Hsueh Y-P. J. Cell Biol 2007;177:829–841. [PubMed: 17548511]
54. Dong JM, Leung T, Manser E, Lim L. J. Biol. Chem 1998;273:22554–22562. [PubMed: 9712882]
55. O'Connor KL, Nguyen B, Mercurio AM. J. Cell Biol 2000;148:253–258. [PubMed: 10648558]
56. Lang P, Gesbert F, Delespine-Carmagnat M, Stancou R, Pouchelet M, Bertoglio J. EMBO J 1996;15:510–519. [PubMed: 8599934]
57. Honjo M, Tanihara H, Inatani M, Kido N, Yue BYJT, Narumiya S, Honda Y. Invest. Ophthalmol. Vis. Sci 2001;42:137–144. [PubMed: 11133858]
58. Rho PV, Deng P-F, Kumar J, Epstein DL. Invest. Ophthalmol. Vis. Sci 2001;42:1029–1037. [PubMed: 11274082]
59. Vittitow JL, Garg R, Rowlette LLS, Epstein DL, O'Brien ET, Borrás T. Mol. Vis 2002;8:32–44. [PubMed: 11889464]
60. Liu X, Hu Y, Filla MS, Gabelt BT, Peters DM, Brandt CR, Kaufman PL. Mol. Vis 2005;11:1112–1121. [PubMed: 16379023]

NIH-PA Author Manuscript
NIH-PA Author Manuscript
NIH-PA Author Manuscript

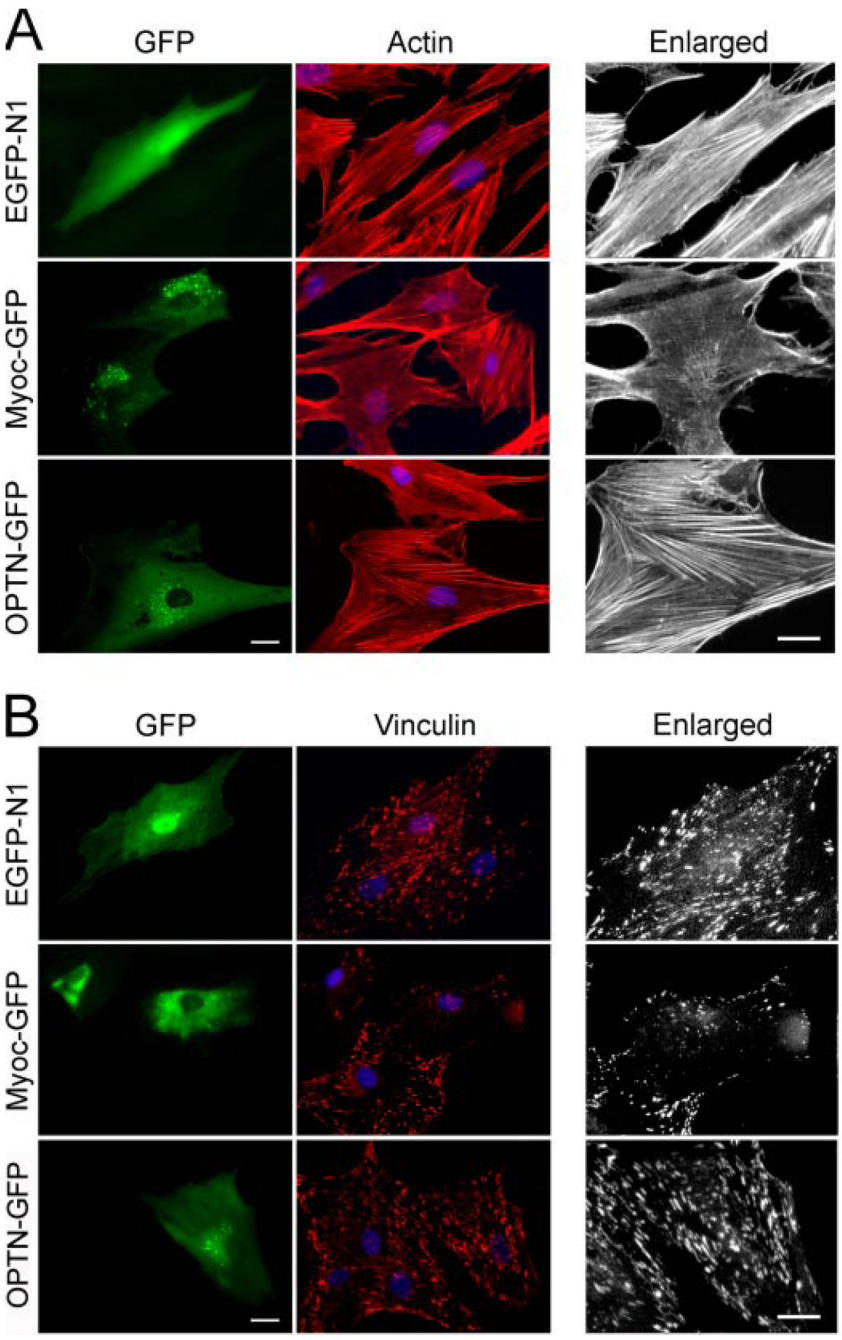

FIGURE 1. Myocilin overexpression induces a loss of actin stress fibers (*A*) and vinculin (*B*) staining
TM cells were transfected with pEGFP-N1 (*EGFP-N1*; mock control), pMyocilin-EGFP (*Myoc-GFP*), or pOptineurin-EGFP (*OPTN-GFP*; a negative control) and stained for actin (*A*, *red*) or vinculin (*B*, *red*). The transfected cells were marked by *green fluorescence*. The enlarged actin and vinculin micrographs of the transfected cells are presented in *black and white*. The staining was visualized using a Zeiss 100M microscope. *Bar*, 20 μm.

NIH-PA Author Manuscript

NIH-PA Author Manuscript

NIH-PA Author Manuscript

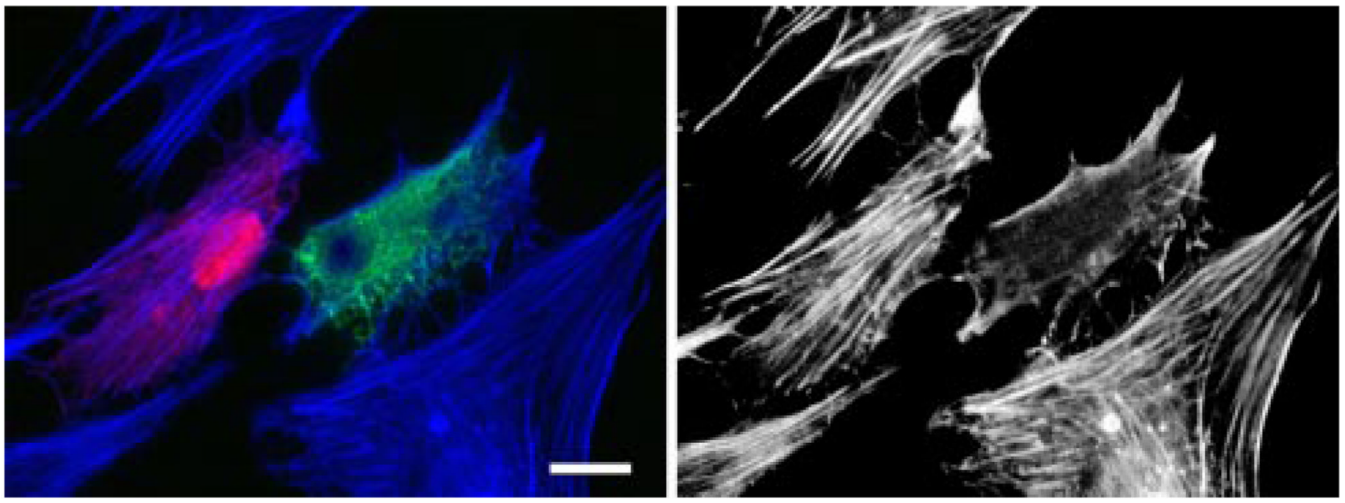

FIGURE 2. Actin staining in mixed cultures of pMyocilin-EGFP- and pDsRed-Monomer-C1-transfected cells

F-actin was stained with Alexa Fluor 350-phalloidin in *blue*. The actin cytoskeleton is shown in *black and white* in the *right panel*. The pMyocilin-EGFP-transfected cell (in *green*) showed a loss of actin stress fibers, whereas the DsRed-expressing (in *red*) and nontransfected cells had robust actin fibers. *Bar*, 20 μm.

NIH-PA Author Manuscript

NIH-PA Author Manuscript

NIH-PA Author Manuscript

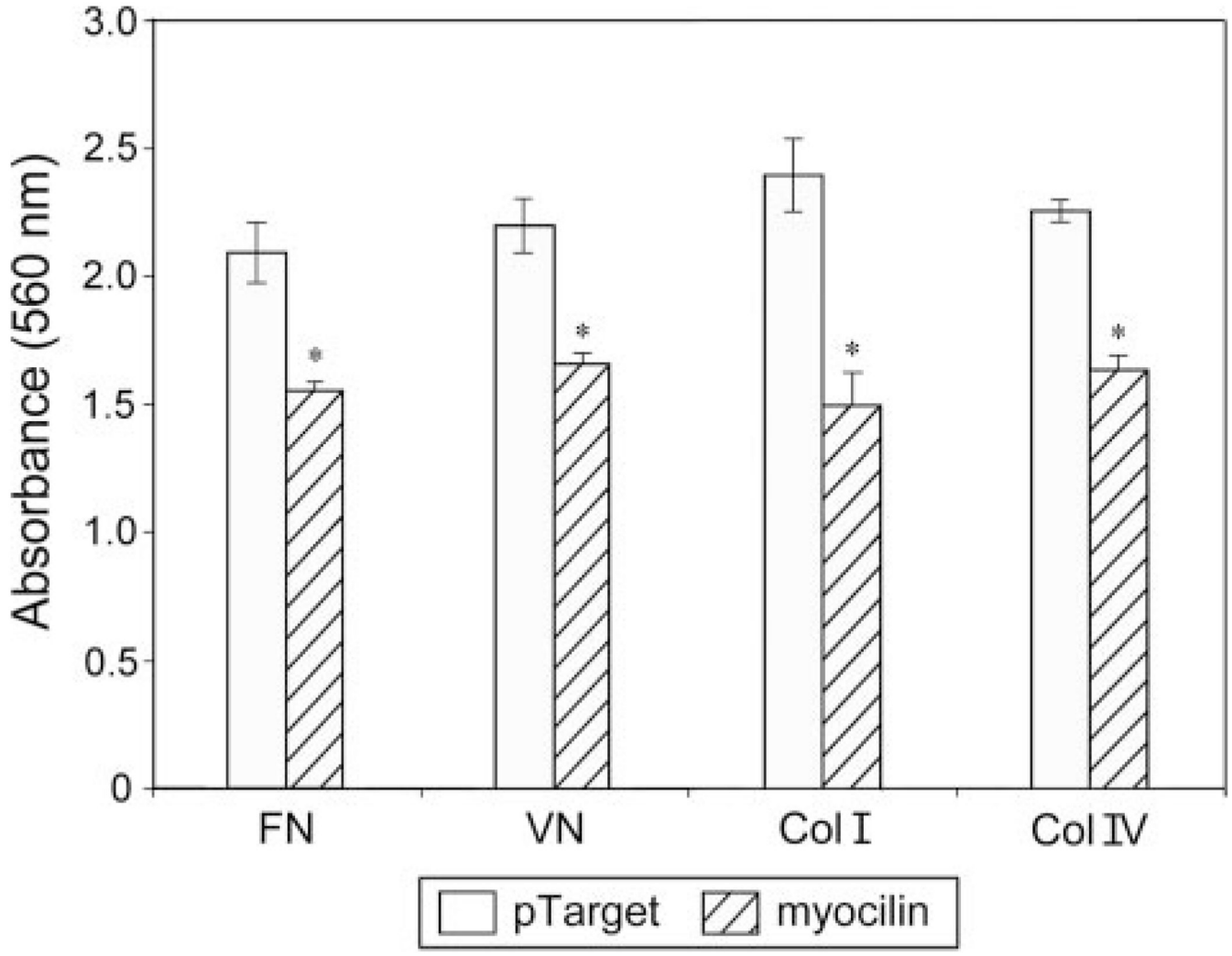

FIGURE 3. Myocilin overexpression impairs TM cell adhesion

Adhesion of pTarget (mock control)- and pTarget-myocilin (*myocilin*)-transfected TM cells was determined using Chemicon CytoMatrix cell adhesion strips coated with fibronectin, vitronectin, and collagen types I and IV. Data are presented as mean ± S.E. ($n = 3$). *Asterisks*, data significantly different from corresponding pTarget mock controls. The p values for fibronectin, vitronectin, and collagen type I and IV were 0.0046, 0.0032, 0.0063, and < 0.0001, respectively.

NIH-PA Author Manuscript
NIH-PA Author Manuscript
NIH-PA Author Manuscript

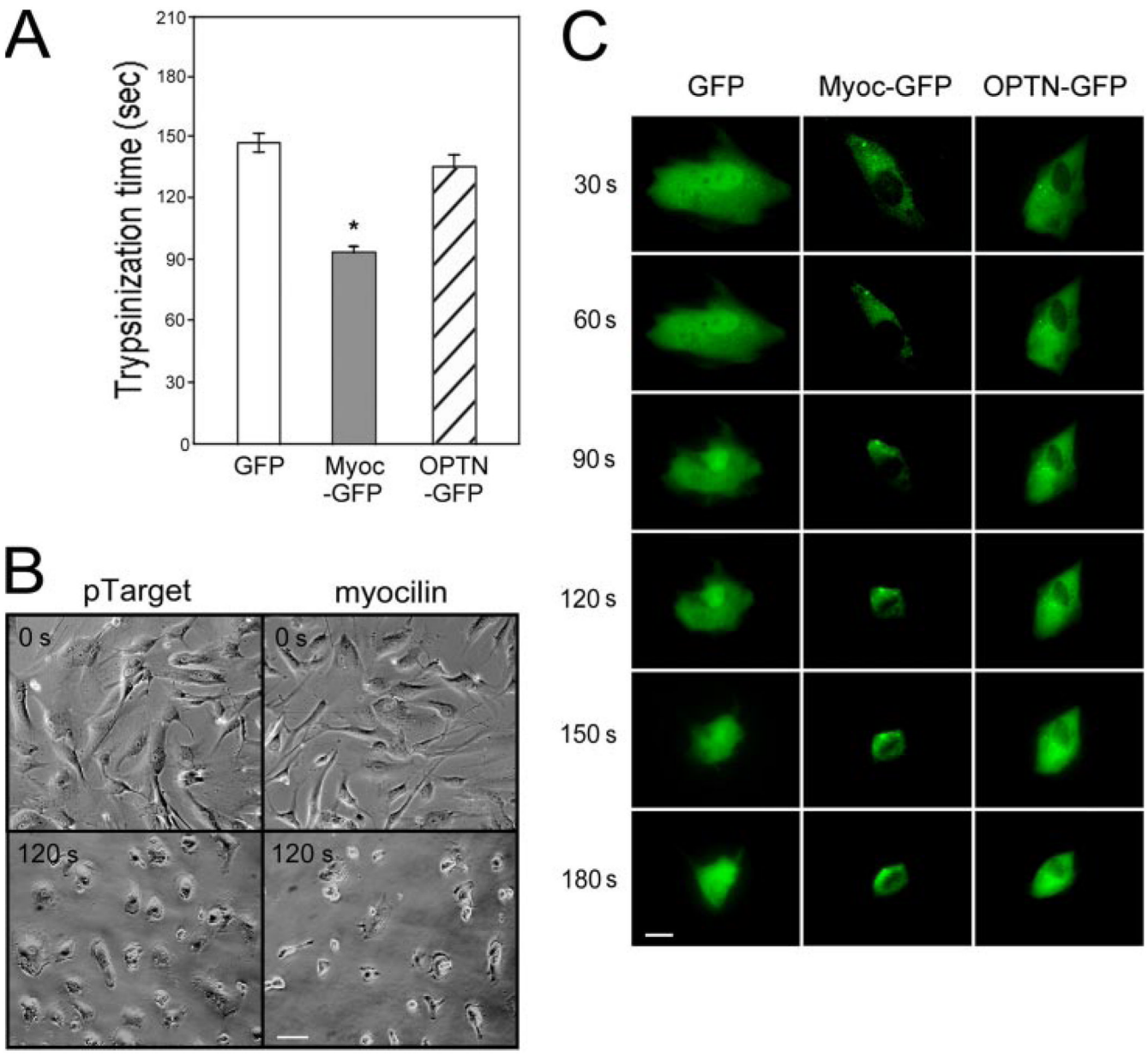

FIGURE 4. Myocilin-transfected cells displayed a heightened sensitivity to trypsinization

A, the trypsinization time needed for pEGFP-N1 (*GFP*)-, pMyocilin-EGFP (*Myoc-GFP*)-, and pOptineurin-EGFP (*OPTN-GFP*)- transfected TM cells to become refractile. *, the trypsinization time for myocilin transfectants was significantly ($p < 0.0001$, $n = 30$) lower than that of GFP or optineurin controls. *B*, phase-contrast micrographs of pTarget- and pTarget-myocilin (myocilin)-transfected cells before (*0 s*) or after trypsinization for 120 s (*120 s*). *Scale bar*, 50 μm. *C*, time lapse video microscopy of pEGFP-N1 (GFP)-, pMyocilin-EGFP (Myoc-EGFP)-, and pOptineurin-EGFP (OPTN-GFP)-transfected cells every 30 s after the addition of trypsin solution to the cultures. *Bar*, 20 μm.

NIH-PA Author Manuscript

NIH-PA Author Manuscript

NIH-PA Author Manuscript

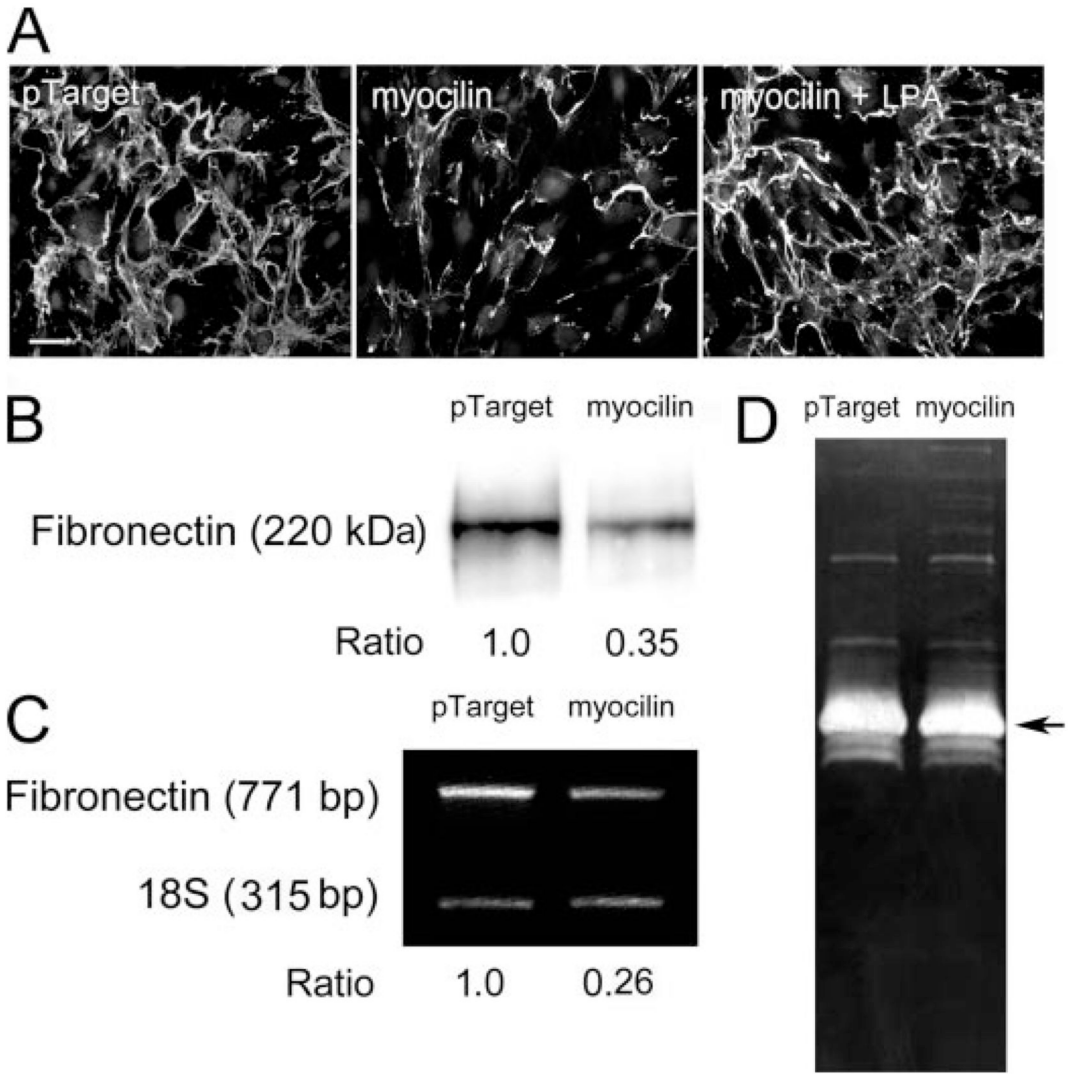

FIGURE 5.

A, effect of myocilin transfection and/or LPA on fibronectin assembly in human TM cultures. Fibronectin (in *green*) assembly in pTarget-transfected, pTarget-myocilin (myocilin)-transfected, and myocilin-transfected and LPA (5 μM, 16 h)-treated (*myocilin + LPA*) TM cells was visualized by immunofluorescence. The nuclei were stained by 4′,6′-diamidino- 2-phenylindole dihydrochloride in *blue*. Experiments were repeated three times, yielding similar results. *Bar*, 50 μm. *B*, secreted fibronectin protein level; *C*, fibronectin transcript level; *D*,MMPactivities in pTarget- and pTarget-myocilin (myocilin)-transfected TM cultures. Fibronectin secretion into the medium was examined by Western blotting (*B*). The level of fibronectin transcript was measured by relative quantitative RT-PCR (*C*). Relative to mock controls, the secreted fibronectin protein and the transcript levels were reduced by ~70%. The MMP activities were visualized by zymography (*D*). Experiments were repeated two times, yielding similar results.

NIH-PA Author Manuscript
NIH-PA Author Manuscript
NIH-PA Author Manuscript

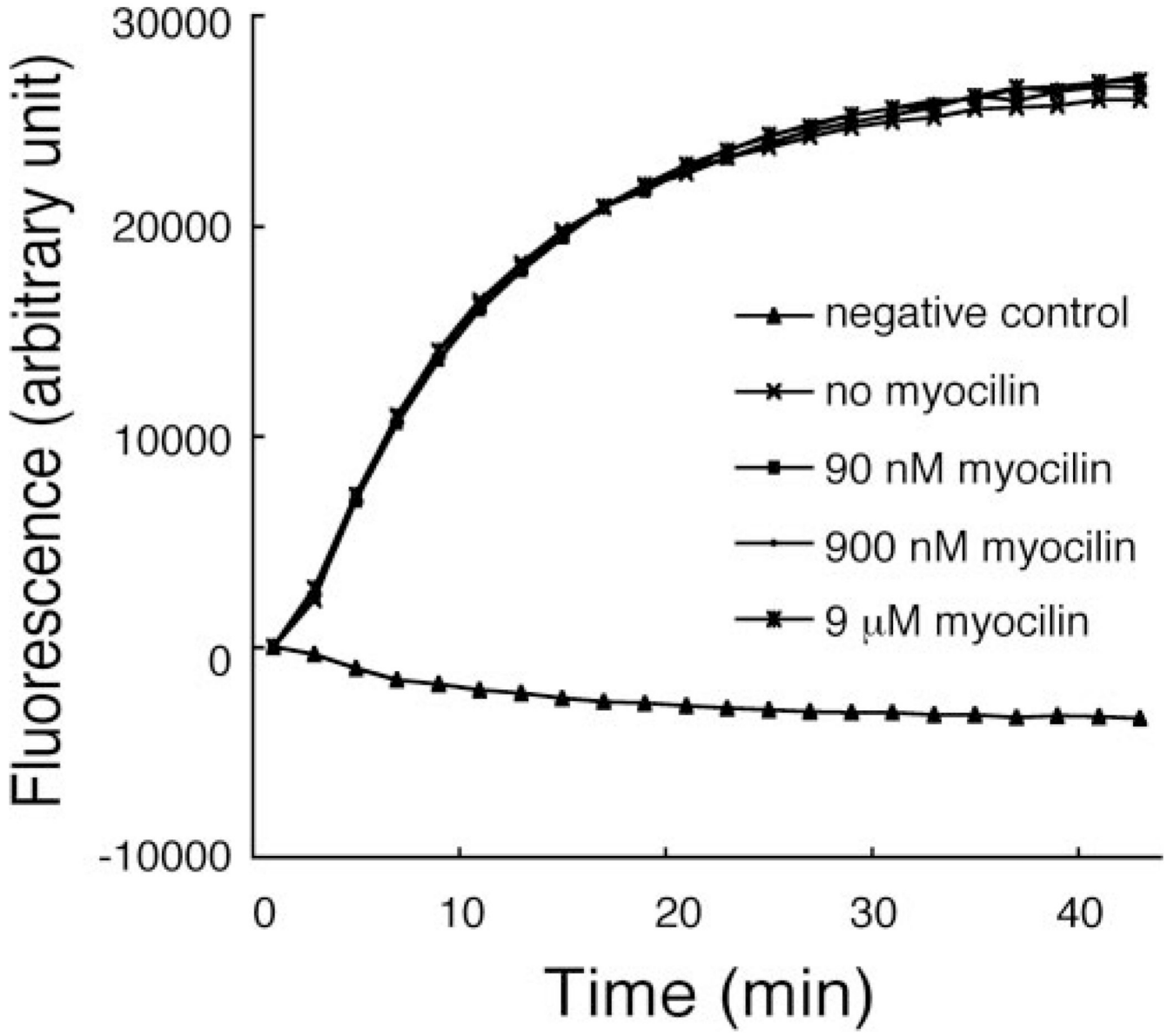

FIGURE 6. Effect of recombinant human myocilin on actin polymerization

In *in vitro* assays, the actin polymerization was induced by actin polymerization buffer in the absence or presence of 90 nM, 900 nM, or 9μM recombinant human myocilin. The actin polymerization buffer was not added to the negative control. Experiments were repeated three times with similar results.

NIH-PA Author Manuscript
NIH-PA Author Manuscript
NIH-PA Author Manuscript

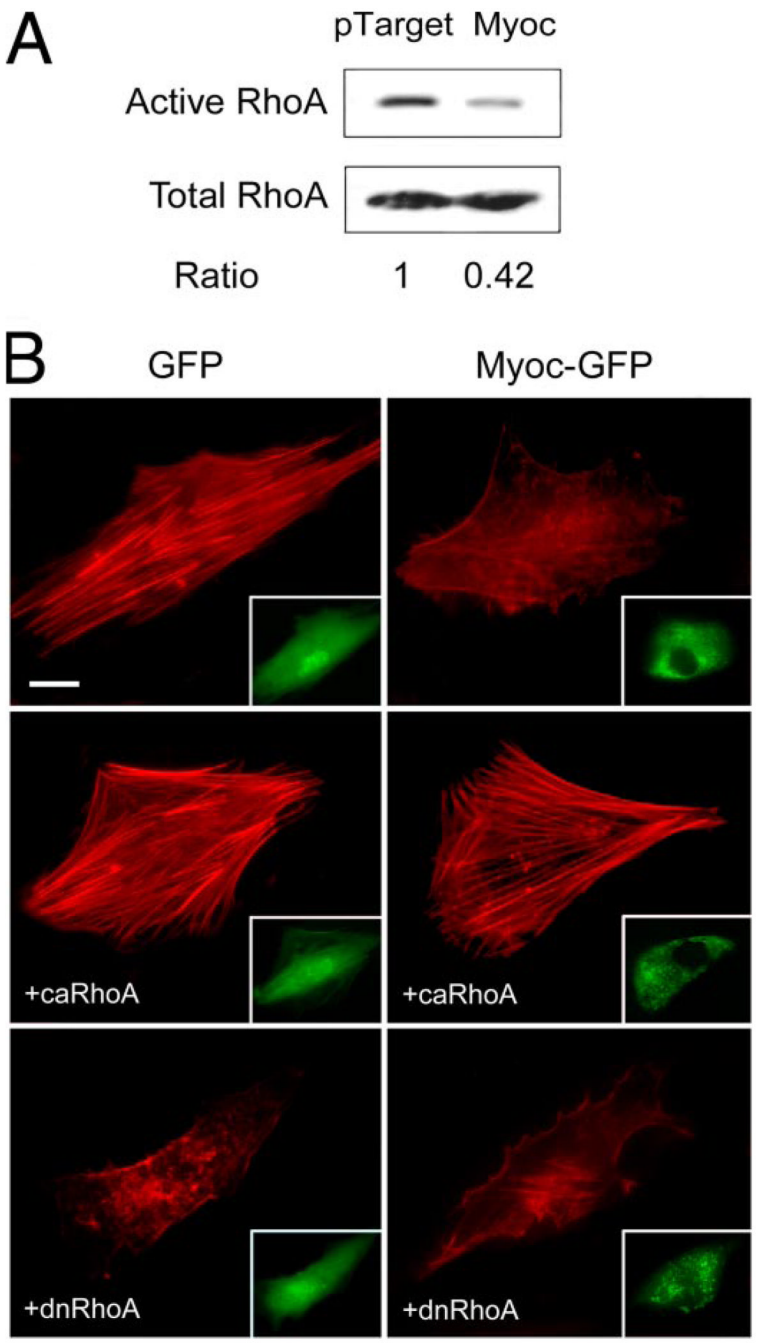

FIGURE 7.

A, GTP-bound active RhoA in pTarget- and pTarget-myocilin (*Myoc*)-transfected TM cells. Pull-down assays were performed to determine the RhoA activity. The amount of the active or GTP-bound RhoA was normalized against the total amount in cell lysates. Data compiled indicated that the RhoA activity upon myocilin transfection (0.55 ± 0.10, $n = 6$) was significantly reduced ($p < 0.007$) compared with controls. *B*, effect of co-expression of ca or dn RhoA in TM cells on the actin cytoskeleton. Human TM cells in culture were transfected with pEGFP-N1 (GFP) or pMyocilin-EGFP (Myoc-GFP) with-out (*top panels*), or with co-transfection with plasmid encoding ca V14 RhoA (+*caRhoA*) or dn N19 RhoA (+*dnRhoA*). The transfected cells displaying green fluorescence are shown in the *insets*. The actin staining

NIH-PA Author Manuscript

NIH-PA Author Manuscript

NIH-PA Author Manuscript

(in *red*) was examined by fluorescence microscopy. Cells transfected with pEGFP-N1 as a control exhibited robust actin stress fibers. Transfection with pMyocilin-EGFP caused a loss of actin fibers. An increase of the actin assembly or rescue of the myocilin phenotype was observed with co-expression of the ca but not dn form of RhoA. *Bar*, 20 μm.

NIH-PA Author Manuscript
NIH-PA Author Manuscript
NIH-PA Author Manuscript

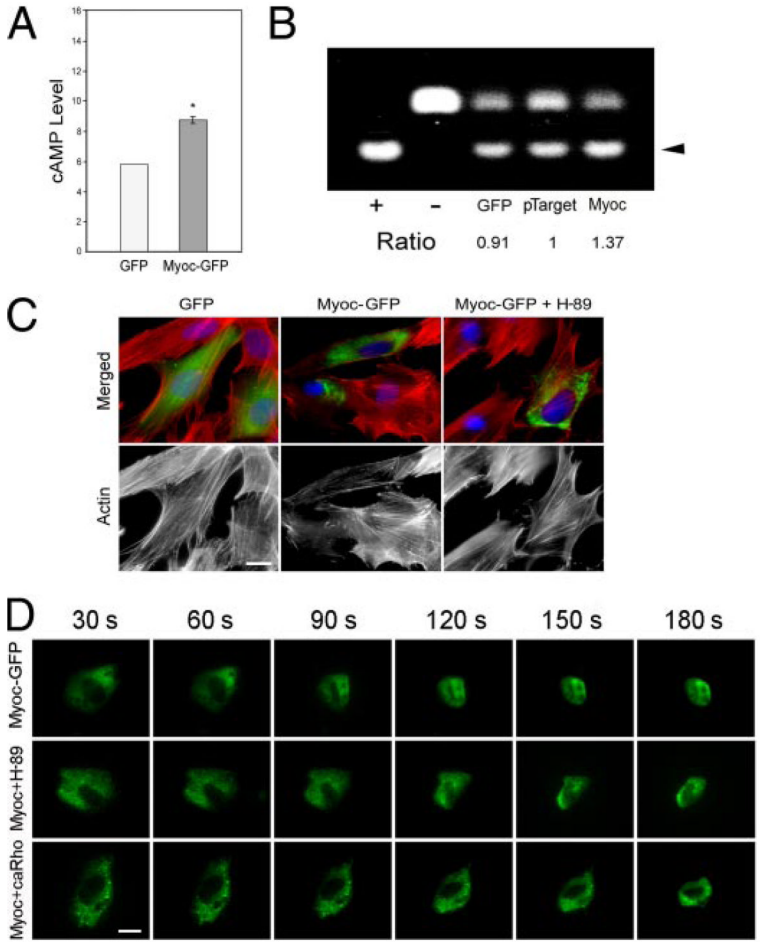

FIGURE 8.

A, cAMP level in pEGFP-N1 (*GFP*)- or pMyocilin-EGFP (*Myoc-GFP*)- transfected TM cells. The cAMP level in myocilin transfectants (1.47 ± 0.03, $n = 4$) measured by an ELISA was expressed relative to the controls. *, the cAMP level for myocilin transfectants was significantly ($p < 0.0037$) increased compared with GFP mock controls. *B*, PKA activity in pEGFP-N1 (*GFP*)-, pTarget-, or pTarget-myocilin (*Myoc*)-transfected cells. Equal amounts of protein lysates were subjected to PKA assays. Positive (+) and negative (−) controls were included. The nonphosphorylated (*upper band*) and the phosphorylated (*lower band*, *arrowhead*) substrates were resolved on agarose gels. The PKA activity, judged by the level of the phosphorylated substrate, in pTarget-myocilin transfectants (1.39 ± 0.02, $n = 9$, $p < 0.0001$) was determined by densitometric analyses and normalized to that in pTarget controls. Results shown are from one of the experiments. *C*, actin staining in pEGF-N1 (*GFP*)- and pMyocilin-EGFP (*Myoc-GFP*)-transfected TM cells without or with the treatment with PKA inhibitor, H-89 (*Myoc + H-89*). *D*, time lapse video microscopy of pMyocilin-EGFP (*Myoc-GFP*)-transfected cells and those with H-89 treatment (Myoc + H-89) or co-transfection with ca RhoA (Myoc + caRho) every 30 s after the addition of trypsin solution to the cultures. *Bar*, 20 μm.

NIH-PA Author Manuscript

NIH-PA Author Manuscript

NIH-PA Author Manuscript

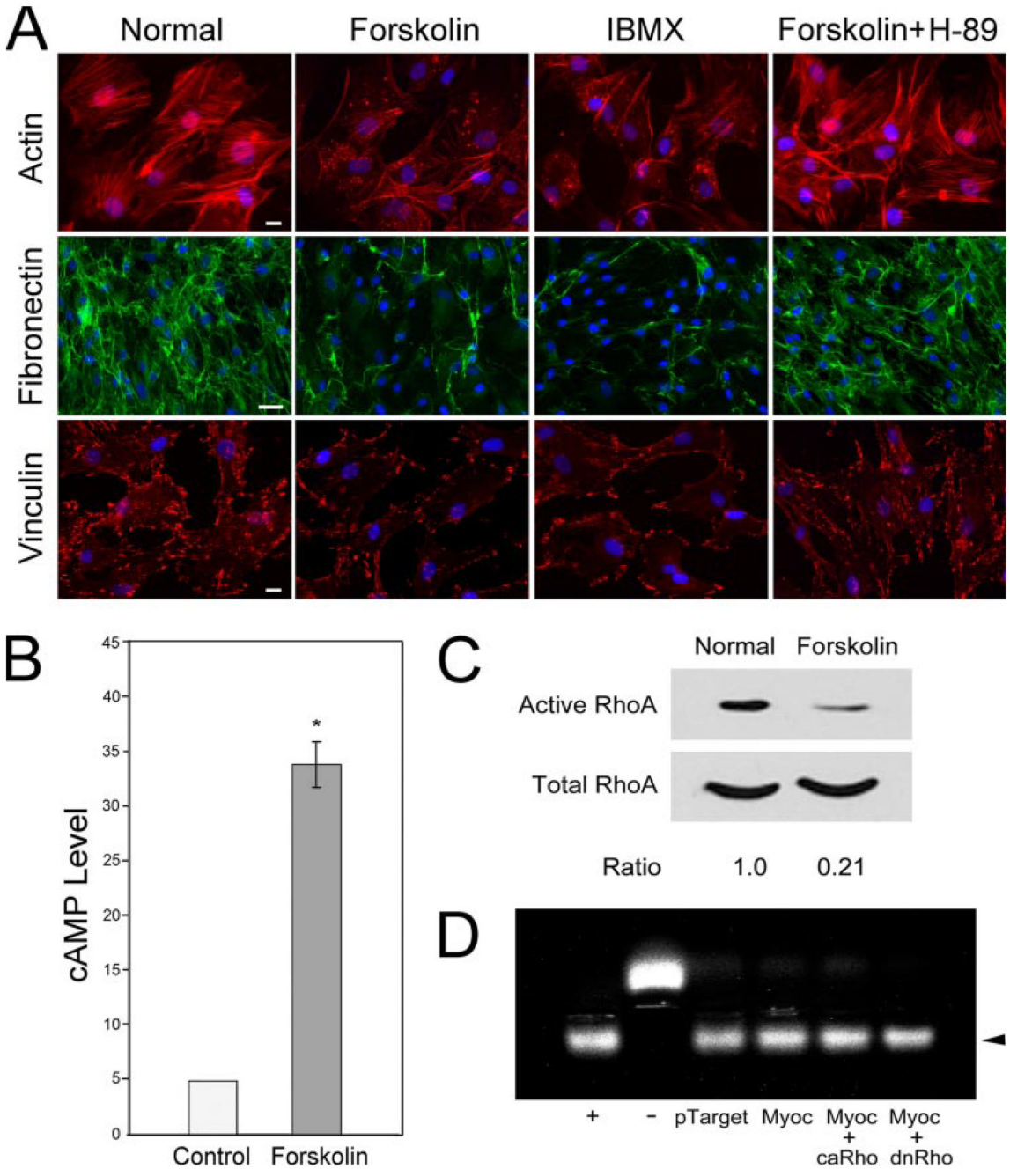

FIGURE 9.

A, actin (*red*), fibronectin (*green*), and vinculin (*red*) staining in normal humanTMcells after overnight treatment with 50 μM forskolin, 500 μM IBMX, or 50 μM forskolin plus 10 nM H-89. The nuclei were stained by 4′,6′-diamidino-2-phenylindole dihydrochloride in *blue*. *Bar* for actin and vinculin, 20 μm; *bar* for fibronectin, 50 μm. *B*, cAMP level was increased by forskolin treatment by ~7-fold (34.0 ± 6.7 *versus* 4.9 ± 0.1; $n = 4$). *C*, inhibition of RhoA activity after forskolin induction ofcAMPin normalhumanTMcells. The experiments were repeated twice. *D*, PKA activity in TM cells transfected with pTarget, pTarget-myocilin (*Myoc*), pTarget-myocilin plus ca RhoA (*Myoc* + *caRho*), or pTarget-myocilin plus dn RhoA (*Myoc* + *dnRho*). Positive (+) and negative (−) controls were included. The PKA activity was determined as

described in the legend to Fig. 8*B*. Results were expressed as ratios relative to the pTarget control. Data from one representative experiment are presented.

NIH-PA Author Manuscript
NIH-PA Author Manuscript
NIH-PA Author Manuscript

NIH-PA Author Manuscript

NIH-PA Author Manuscript

NIH-PA Author Manuscript

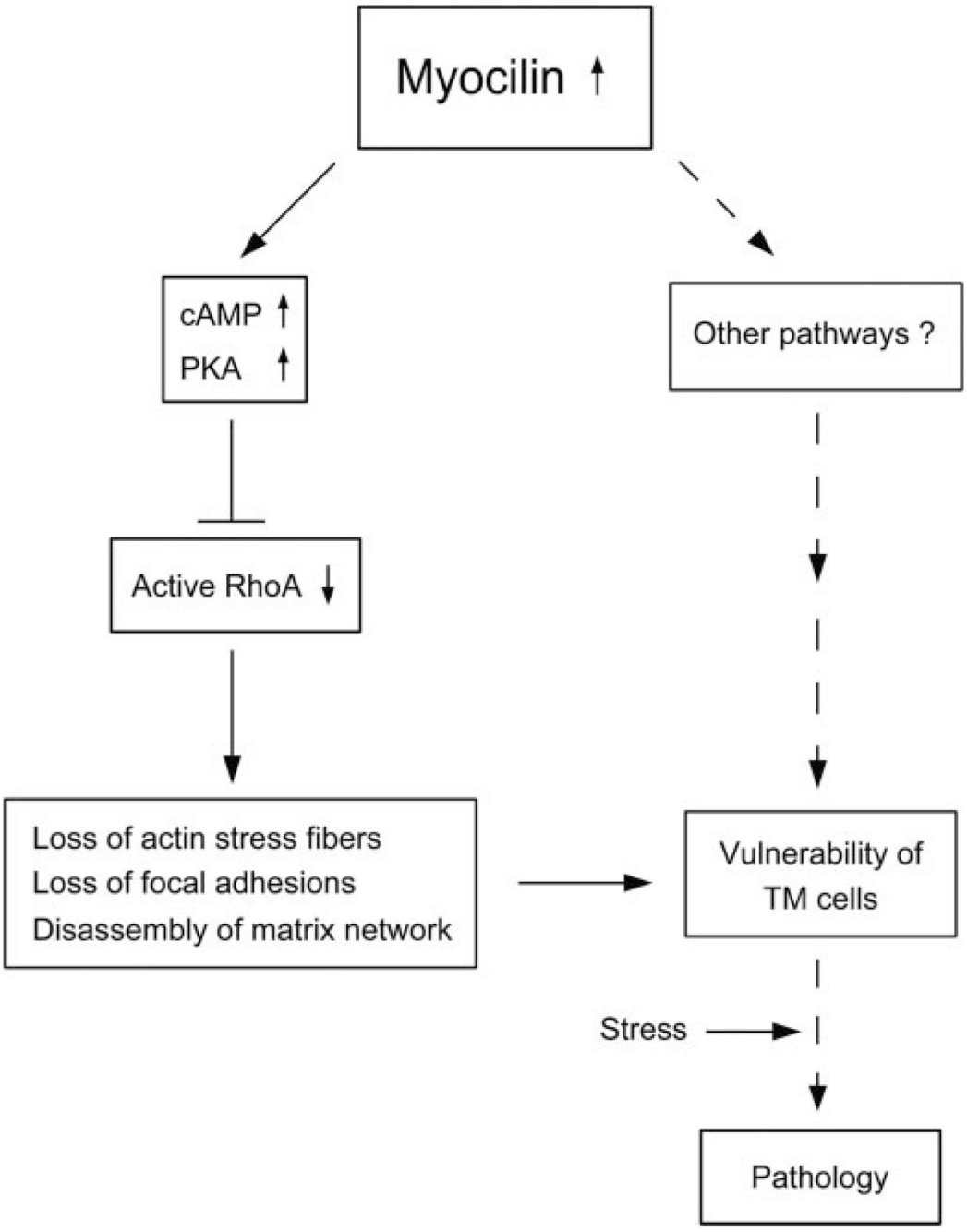

FIGURE 10. A working model of possible events in human TM cells triggered by up-regulation of myocilin

Myocilin, when moderately up-regulated, induces cAMP/PKA activation and the downstream RhoA inactivation, leading to a loss of actin stress fibers and focal adhesions and disassembly of matrix network. These changes or other pathways may affect the integrity of TM cells, rendering them more susceptible to additional stress or challenge and pathologic consequences. Other intermediate mediators or pathways have yet to be identified. The *dotted lines* indicate steps that have not been investigated in the present work or in our previous investigation (17).